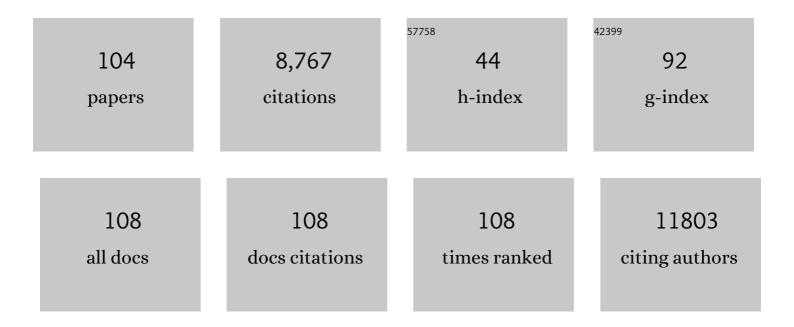
Guoliang Liu

List of Publications by Year in descending order

Source: https://exaly.com/author-pdf/5639478/publications.pdf Version: 2024-02-01



#	Article	IF	CITATIONS
1	Porous Carbon Nanofiber-Modified Carbon Fiber Microelectrodes for Dopamine Detection. ACS Applied Nano Materials, 2022, 5, 2241-2249.	5.0	16
2	Block Copolymerâ€Derived Porous Carbon Fibers Enable High MnO ₂ Loading and Fast Charging in Aqueous Zincâ€Ion Battery. Batteries and Supercaps, 2022, 5, .	4.7	9
3	Physics and chemistry-based constitutive modeling of photo-oxidative aging in semi-crystalline polymers. International Journal of Solids and Structures, 2022, 239-240, 111427.	2.7	6
4	Can the Voigt Model be Directly Used for Determining the Modulus of Graphene in Laminate Thin Films?. ACS Applied Polymer Materials, 2022, 4, 394-402.	4.4	2
5	Utilization of Block Copolymers to Understand Water Vaporization Enthalpy Reduction in Uniform Pores. Macromolecules, 2022, 55, 4803-4811.	4.8	5
6	Humidity-Controlled Preparation of Flexible Porous Carbon Fibers from Block Copolymers. ACS Applied Polymer Materials, 2022, 4, 4980-4992.	4.4	6
7	Covalent and Noncovalent Loading of Doxorubicin by Folic Acid-Carbon Dot Nanoparticles for Cancer Theranostics. ACS Omega, 2022, 7, 23322-23331.	3.5	10
8	Mutually Reinforced Polymer–Graphene Bilayer Membranes for Energyâ€Efficient Acoustic Transduction. Advanced Materials, 2021, 33, e2004053.	21.0	9
9	Solvent-Resistant Self-Crosslinked Poly(ether imide). Macromolecules, 2021, 54, 3405-3412.	4.8	16
10	Recent development of polyimides: Synthesis, processing, and application in gas separation. Journal of Polymer Science, 2021, 59, 943-962.	3.8	43
11	Poly(ether imide)s with tailored end groups. Journal of Polymer Science, 2021, 59, 2365.	3.8	2
12	Mesoporous polyetherimide thin films <i>via</i> hydrolysis of polylactide- <i>b</i> -polyetherimide- <i>b</i> -polylactide. Polymer Chemistry, 2021, 12, 3939-3946.	3.9	2
13	Controlling the physical and electrochemical properties of block copolymer-based porous carbon fibers by pyrolysis temperature. Molecular Systems Design and Engineering, 2020, 5, 153-165.	3.4	34
14	Impact of metal cations on the thermal, mechanical, and rheological properties of telechelic sulfonated polyetherimides. Polymer Chemistry, 2020, 11, 393-400.	3.9	10
15	Facile Preparation of Halogen-Free Poly(ether imide) Containing Phosphonium and Sulfonate Groups. ACS Applied Polymer Materials, 2020, 2, 66-73.	4.4	4
16	Porous organic materials offer vast future opportunities. Nature Communications, 2020, 11, 4984.	12.8	39
17	Molecular-Level Control over Plasmonic Properties in Silver Nanoparticle/Self-Assembling Peptide Hybrids. Journal of the American Chemical Society, 2020, 142, 9158-9162.	13.7	26
18	A Review on Nano-/Microstructured Materials Constructed by Electrochemical Technologies for Supercapacitors. Nano-Micro Letters, 2020, 12, 118.	27.0	146

#	Article	IF	CITATIONS
19	Capacitive Organic Dye Removal by Block Copolymer Based Porous Carbon Fibers. Advanced Materials Interfaces, 2020, 7, 2000507.	3.7	11
20	Addressing the Achilles' heel of pseudocapacitive materials: Longâ€ŧerm stability. InformaÄnÃ-Materiály, 2020, 2, 807-842.	17.3	135
21	Overlooking Issues and Prospective Resolutions Behind the Prosperity of Three-Dimensional Porous Carbon Supercapacitor Electrodes. Frontiers in Energy Research, 2020, 8, .	2.3	3
22	Thermally Stable and Mechanically Strong Mesoporous Films of Poly(ether imide)-Based Triblock Copolymers. ACS Applied Polymer Materials, 2020, 2, 1398-1405.	4.4	11
23	Exceptional capacitive deionization rate and capacity by block copolymer–based porous carbon fibers. Science Advances, 2020, 6, eaaz0906.	10.3	108
24	Cobalt-Containing Nanoporous Nitrogen-Doped Carbon Nanocuboids from Zeolite Imidazole Frameworks for Supercapacitors. Nanomaterials, 2019, 9, 1110.	4.1	21
25	Block copolymer-based porous carbons for supercapacitors. Journal of Materials Chemistry A, 2019, 7, 23476-23488.	10.3	74
26	Zipping Up NiFe(OH) _{<i>x</i>} -Encapsulated Hematite To Achieve an Ultralow Turn-On Potential for Water Oxidation. ACS Energy Letters, 2019, 4, 1983-1990.	17.4	82
27	Composition Design of Block Copolymers for Porous Carbon Fibers. Chemistry of Materials, 2019, 31, 8898-8907.	6.7	31
28	Sub-10 nm domains in high-performance polyetherimides. Polymer Chemistry, 2019, 10, 379-385.	3.9	15
29	Mechanically Strong, Thermally Stable, and Flame Retardant Poly(ether imide) Terminated with Phosphonium Bromide. Macromolecules, 2019, 52, 7361-7368.	4.8	14
30	Block copolymer–based porous carbon fibers. Science Advances, 2019, 5, eaau6852.	10.3	201
31	Nanostructure stability and swelling of ternary block copolymer/homopolymer blends: A direct comparison between dissipative particle dynamics and experiment. Journal of Polymer Science, Part B: Polymer Physics, 2019, 57, 794-803.	2.1	12
32	Spectral-Selective Plasmonic Polymer Nanocomposites Across the Visible and Near-Infrared. ACS Nano, 2019, 13, 4255-4266.	14.6	12
33	Pore and Heteroatom Engineered Carbon Foams for Supercapacitors. Advanced Energy Materials, 2019, 9, 1803665.	19.5	321
34	The potassium hydroxide-urea synergy in improving the capacitive energy-storage performance of agar-derived carbon aerogels. Carbon, 2019, 147, 451-459.	10.3	46
35	Critical Role of Polystyrene Layer on Plasmonic Silver Nanoplates in Organic Photovoltaics. ACS Applied Energy Materials, 2019, 2, 2475-2485.	5.1	4
36	A silver wire aerogel promotes hydrogen peroxide reduction for fuel cells and electrochemical sensors. Journal of Materials Chemistry A, 2019, 7, 11497-11505.	10.3	32

#	Article	IF	CITATIONS
37	Block copolymers for supercapacitors, dielectric capacitors and batteries. Journal of Physics Condensed Matter, 2019, 31, 233001.	1.8	27
38	Block copolymer derived uniform mesopores enable ultrafast electron and ion transport at high mass loadings. Nature Communications, 2019, 10, 675.	12.8	213
39	Aligned continuous cylindrical pores derived from electrospun polymer fibers in titanium diboride. International Journal of Applied Ceramic Technology, 2019, 16, 802-813.	2.1	9
40	Generating Electricity on Chips: Microfluidic Biofuel Cells in Perspective. Industrial & Engineering Chemistry Research, 2018, 57, 2746-2758.	3.7	22
41	Stereoselective photoredox ring-opening polymerization of O-carboxyanhydrides. Nature Communications, 2018, 9, 1559.	12.8	51
42	The Effect of End Group and Molecular Weight on the Yellowness of Polyetherimide. Macromolecular Rapid Communications, 2018, 39, e1800045.	3.9	11
43	Nitrogen-doped carbon "spider webs―derived from pyrolysis of polyaniline nanofibers in ammonia for capacitive energy storage. Journal of Materials Research, 2018, 33, 1109-1119.	2.6	16
44	Preferred domain orientation in block copolymer fibers after solvent annealing. Molecular Systems Design and Engineering, 2018, 3, 357-363.	3.4	8
45	Reduced graphene oxide modified activated carbon for improving power generation of air-cathode microbial fuel cells. Journal of Materials Research, 2018, 33, 1279-1287.	2.6	8
46	Melt-processable telechelic poly(ether imide)s end-capped with zinc sulfonate salts. Polymer Chemistry, 2018, 9, 5660-5670.	3.9	8
47	Janus Plasmonic Silver Nanoplatelets for Interface Stabilization. ACS Applied Nano Materials, 2018, 1, 5377-5381.	5.0	9
48	Boosting the Power-Generation Performance of Micro-Sized Al-H2O2 Fuel Cells by Using Silver Nanowires as the Cathode. Energies, 2018, 11, 2316.	3.1	6
49	Direct ink writing of organic and carbon aerogels. Materials Horizons, 2018, 5, 1166-1175.	12.2	78
50	Tuning the Electrochemical Properties of Nitrogen-Doped Carbon Aerogels in a Blend of Ammonia and Nitrogen Gases. ACS Applied Energy Materials, 2018, 1, 5043-5053.	5.1	21
51	Engineering of Mesoscale Pores in Balancing Mass Loading and Rate Capability of Hematite Films for Electrochemical Capacitors. Advanced Energy Materials, 2018, 8, 1801784.	19.5	97
52	Controlling the Pore Size of Mesoporous Carbon Thin Films through Thermal and Solvent Annealing. Small, 2017, 13, 1603107.	10.0	43
53	Low-Molecular-Weight, High-Mechanical-Strength, and Solution-Processable Telechelic Poly(ether) Tj ETQq1 1 0	.784314 rş 4.8	gBT_/Overloc
54	Multiscale Pore Network Boosts Capacitance of Carbon Electrodes for Ultrafast Charging. Nano	9.1	251

Letters, 2017, 17, 3097-3104.

9.1 251

#	Article	IF	CITATIONS
55	Two-Dimensional Plasmonic Nanoparticle as a Nanoscale Sensor to Probe Polymer Brush Formation. Analytical Chemistry, 2017, 89, 7541-7548.	6.5	13
56	Progress in Developing Metal Oxide Nanomaterials for Photoelectrochemical Water Splitting. Advanced Energy Materials, 2017, 7, 1700555.	19.5	455
57	Improved block copolymer domain dispersity on chemical patterns via homopolymer-blending and molecular transfer printing. Polymer, 2017, 116, 99-104.	3.8	5
58	Morphology and Doping Engineering of Sn-Doped Hematite Nanowire Photoanodes. Nano Letters, 2017, 17, 2490-2495.	9.1	204
59	Drug-Loaded Polymeric Spherical Nucleic Acids: Enhancing Colloidal Stability and Cellular Uptake of Polymeric Nanoparticles through DNA Surface-Functionalization. Biomacromolecules, 2017, 18, 483-489.	5.4	47
60	Poly(vinylpyrrolidone)â€Free Multistep Synthesis of Silver Nanoplates with Plasmon Resonance in the Near Infrared Range. Small, 2017, 13, 1701715.	10.0	23
61	Recent advances in chemical methods for activating carbon and metal oxide based electrodes for supercapacitors. Journal of Materials Chemistry A, 2017, 5, 17151-17173.	10.3	135
62	Revitalizing carbon supercapacitor electrodes with hierarchical porous structures. Journal of Materials Chemistry A, 2017, 5, 17705-17733.	10.3	464
63	3D Printed Functionally Graded Plasmonic Constructs. Advanced Optical Materials, 2017, 5, 1700367.	7.3	37
64	Ostwald Ripening Improves Rate Capability of High Mass Loading Manganese Oxide for Supercapacitors. ACS Energy Letters, 2017, 2, 1752-1759.	17.4	146
65	3D printed functional nanomaterials for electrochemical energy storage. Nano Today, 2017, 15, 107-120.	11.9	302
66	Hierarchically porous carbon foams for electric double layer capacitors. Nano Research, 2016, 9, 2875-2888.	10.4	120
67	A three-dimensional nitrogen-doped graphene aerogel-activated carbon composite catalyst that enables low-cost microfluidic microbial fuel cells with superior performance. Journal of Materials Chemistry A, 2016, 4, 15913-15919.	10.3	68
68	Key Parameter Controlling the Sensitivity of Plasmonic Metal Nanoparticles: Aspect Ratio. Journal of Physical Chemistry C, 2016, 120, 19353-19364.	3.1	56
69	Plasmonic solar desalination. Nature Photonics, 2016, 10, 361-362.	31.4	35
70	Supercapacitors Based on Three-Dimensional Hierarchical Graphene Aerogels with Periodic Macropores. Nano Letters, 2016, 16, 3448-3456.	9.1	608
71	Using Scanning-Probe Block Copolymer Lithography and Electron Microscopy To Track Shape Evolution in Multimetallic Nanoclusters. ACS Nano, 2015, 9, 12137-12145.	14.6	21
72	Tip-Directed Synthesis of Multimetallic Nanoparticles. Journal of the American Chemical Society, 2015, 137, 9167-9173.	13.7	136

#	Article	IF	CITATIONS
73	An Electrochemical Capacitor with Applicable Energy Density of 7.4 Wh/kg at Average Power Density of 3000 W/kg. Nano Letters, 2015, 15, 3189-3194.	9.1	118
74	Photohole Induced Corrosion of Titanium Dioxide: Mechanism and Solutions. Nano Letters, 2015, 15, 7051-7057.	9.1	57
75	Assembly of Supramolecular Nanotubes from Molecular Triangles and 1,2-Dihalohydrocarbons. Journal of the American Chemical Society, 2014, 136, 16651-16660.	13.7	81
76	A New Benchmark Capacitance for Supercapacitor Anodes by Mixedâ€Valence Sulfurâ€Doped V ₆ O _{13â^'<i>x</i>} . Advanced Materials, 2014, 26, 5869-5875.	21.0	305
77	Polyaniline and Polypyrrole Pseudocapacitor Electrodes with Excellent Cycling Stability. Nano Letters, 2014, 14, 2522-2527.	9.1	688
78	Improving the Cycling Stability of Metal–Nitride Supercapacitor Electrodes with a Thin Carbon Shell. Advanced Energy Materials, 2014, 4, 1300994.	19.5	217
79	Desktop nanofabrication with massively multiplexed beam pen lithography. Nature Communications, 2013, 4, 2103.	12.8	86
80	Anisotropic Nanoparticles as Shape-Directing Catalysts for the Chemical Etching of Silicon. Journal of the American Chemical Society, 2013, 135, 12196-12199.	13.7	44
81	The role of viscosity on polymer ink transport in dip-pen nanolithography. Chemical Science, 2013, 4, 2093.	7.4	44
82	A cantilever-free approach to dot-matrix nanoprinting. Proceedings of the National Academy of Sciences of the United States of America, 2013, 110, 12921-12924.	7.1	33
83	Selective isolation of gold facilitated by second-sphere coordination with α-cyclodextrin. Nature Communications, 2013, 4, 1855.	12.8	156
84	A general approach to DNA-programmable atom equivalents. Nature Materials, 2013, 12, 741-746.	27.5	279
85	Layer-by-Layer Assembly of a Metallomesogen by Dip-Pen Nanolithography. ACS Nano, 2013, 7, 2602-2609.	14.6	21
86	Delineating the pathways for the site-directed synthesis of individual nanoparticles on surfaces. Proceedings of the National Academy of Sciences of the United States of America, 2013, 110, 887-891.	7.1	78
87	Directed Assembly of Non-equilibrium ABA Triblock Copolymer Morphologies on Nanopatterned Substrates. ACS Nano, 2012, 6, 5440-5448.	14.6	50
88	Hollow Spherical Nucleic Acids for Intracellular Gene Regulation Based upon Biocompatible Silica Shells. Nano Letters, 2012, 12, 3867-3871.	9.1	111
89	Morphology of Lamellae-Forming Block Copolymer Films between Two Orthogonal Chemically Nanopatterned Striped Surfaces. Physical Review Letters, 2012, 108, 065502.	7.8	34
90	Symmetric Diblock Copolymers Confined by Two Nanopatterned Surfaces. Macromolecules, 2012, 45, 2588-2596.	4.8	25

#	Article	IF	CITATIONS
91	Nonbulk Complex Structures in Thin Films of Symmetric Block Copolymers on Chemically Nanopatterned Surfaces. Macromolecules, 2012, 45, 3986-3992.	4.8	40
92	Fabrication of chevron patterns for patterned media with block copolymer directed assembly. Journal of Vacuum Science and Technology B:Nanotechnology and Microelectronics, 2011, 29, 06F204.	1.2	14
93	Cross-sectional Imaging of Block Copolymer Thin Films on Chemically Patterned Surfaces. Journal of Photopolymer Science and Technology = [Fotoporima Konwakai Shi], 2010, 23, 149-154.	0.3	14
94	Integration of Density Multiplication in the Formation of Deviceâ€Oriented Structures by Directed Assembly of Block Copolymer–Homopolymer Blends. Advanced Functional Materials, 2010, 20, 1251-1257.	14.9	99
95	Mechanism and dynamics of block copolymer directed assembly with density multiplication on chemically patterned surfaces. Journal of Vacuum Science and Technology B:Nanotechnology and Microelectronics, 2010, 28, C6B13-C6B19.	1.2	10
96	Molecular Transfer Printing Using Block Copolymers. ACS Nano, 2010, 4, 599-609.	14.6	69
97	Interpolation in the Directed Assembly of Block Copolymers on Nanopatterned Substrates: Simulation and Experiments. Macromolecules, 2010, 43, 3446-3454.	4.8	131
98	Modification of a polystyrene brush layer by insertion of poly(methyl methacrylate) molecules. Journal of Vacuum Science & Technology B, 2009, 27, 3038-3042.	1.3	18
99	Dimensional Scaling of Cylinders in Thin Films of Block Copolymerâ^'Homopolymer Ternary Blends. Macromolecules, 2009, 42, 5139-5145.	4.8	49
100	Phase Behavior and Dimensional Scaling of Symmetric Block Copolymerâ^'Homopolymer Ternary Blends in Thin Films. Macromolecules, 2009, 42, 3063-3072.	4.8	63
101	Preparation of Neutral Wetting Brushes for Block Copolymer Films from Homopolymer Blends. Advanced Materials, 2008, 20, 3054-3060.	21.0	74
102	In situ characterization of block copolymer ordering on chemically nanopatterned surfaces by time-resolved small angle x-ray scattering. Journal of Vacuum Science & Technology B, 2008, 26, 2504-2508.	1.3	7
103	Directed Self-Assembly of Block Copolymers for Nanolithography: Fabrication of Isolated Features and Essential Integrated Circuit Geometries. ACS Nano, 2007, 1, 168-175.	14.6	424
104	Enhanced Mechanical Properties of Natural Rubber by Block Copolymer-Based Porous Carbon Fibers. ACS Applied Polymer Materials, 0, , .	4.4	6